

Kadam, R., Zilli, M., Maas, M., Rezwan, K.

### Nanoscale Janus Particles with Dual Protein Functionalization

Journal Article as: peer-reviewed accepted version (Postprint)

DOI of this document\* (secondary publication): <https://doi.org/10.26092/elib/2630>

Publication date of this document: 04/12/2023

\* for better findability or for reliable citation

### Recommended Citation (primary publication/Version of Record) incl. DOI:

Kadam, R., Zilli, M., Maas, M., Rezwan, K., Nanoscale Janus Particles with Dual Protein Functionalization, Part. Part. Syst. Charact. 2018, 35, 1700332. <https://doi.org/10.1002/ppsc.201700332>

Please note that the version of this document may differ from the final published version (Version of Record/primary publication) in terms of copy-editing, pagination, publication date and DOI. Please cite the version that you actually used. Before citing, you are also advised to check the publisher's website for any subsequent corrections or retractions (see also <https://retractionwatch.com/>).

"This is the peer reviewed version of the following article: Kadam, R., Zilli, M., Maas, M., Rezwan, K., Nanoscale Janus Particles with Dual Protein Functionalization, Part. Part. Syst. Charact. 2018, 35, 1700332. <https://doi.org/10.1002/ppsc.201700332>, which has been published in final form at <https://doi.org/10.1002/ppsc.201700332>. This article may be used for non-commercial purposes in accordance with Wiley Terms and Conditions for Use of Self-Archived Versions. This article may not be enhanced, enriched or otherwise transformed into a derivative work, without express permission from Wiley or by statutory rights under applicable legislation. Copyright notices must not be removed, obscured or modified. The article must be linked to Wiley's version of record on Wiley Online Library and any embedding, framing or otherwise making available the article or pages thereof by third parties from platforms, services and websites other than Wiley Online Library must be prohibited."

This document is made available with all rights reserved.

### Take down policy

If you believe that this document or any material on this site infringes copyright, please contact [publizieren@suub.uni-bremen.de](mailto:publizieren@suub.uni-bremen.de) with full details and we will remove access to the material.

# Nanoscale Janus Particles with Dual Protein Functionalization

Reshma Kadam, Marina Zilli, Michael Maas,\* and Kuroschi Rezwan

Biofunctionalized Janus particles with tailored surface chemistry are gathering interest for applications as catalysts, multifunctional cell surface targets, nanomotors, and drug delivery systems. The dual nature of the surface chemistry of Janus particles can be exploited to immobilize drugs, cell surface targets, and/or other functional molecules on both sides of the particle surface. In this study, a model system is established for the scalable preparation of nanoscale Janus particles with dual protein functionalization with the proteins ferritin and streptavidin. 80 nm silica nanoparticles (SiNPs) modified with azidosilane are used to prepare Pickering emulsions with molten wax as the droplet phase. The azide-functionalized SiNPs on the Pickering emulsion droplets are further subjected to face-selective silanization with biotin-polyethylene glycol ethoxy silane. Afterward, ferritin is grafted on the azide-functionalized side via a click-reaction and the biotin groups are conjugated with streptavidin which is labeled with ultrasmall gold nanoparticles. In order to elucidate the advantages and limits of this approach, a detailed characterization is performed of the particles at every process step. The results show that this method represents a scalable platform for the versatile preparation of nanoscale Janus nanoparticles that can potentially be used with a wide variety of proteins.

## 1. Introduction

The concept of Janus particles, which was first introduced by Nobel laureate Pierre de Gennes in his acceptance speech in 1991,<sup>[1]</sup> is defined by spatially separated surface functionalities on a single nanoparticle with dual faces and thus enables dual functionalization of colloidal particles on separate sides. Biofunctional Janus particles are emerging tools in cell targeting,<sup>[2]</sup> imaging,<sup>[3]</sup> manipulation of cell immune response,<sup>[4]</sup> and are particularly promising for tailoring cell membrane interactions due to their inherent amphiphilicity.<sup>[5]</sup> For use in applications at the nano-bio interface, Janus nanoparticles need to be functionalized with biological ligands, such as proteins. Homogenous chemical

surface functionalization of nanoparticles has been widely reported in the last years with numerous possible industrial and biotechnological applications,<sup>[6]</sup> while combining multiple surface features have recently gained importance to enable functions such as dual targeting or the combination of properties for both targeting and diagnostics in theranostic nanomedicine.<sup>[6c,7]</sup> Functionalizing Janus particles with two different proteins would allow the combination of otherwise incompatible proteins on a single nanoparticle surface and would thus enable advanced applications in targeting, signaling, or a similar combination of functions.<sup>[8]</sup>

While the preparation of biofunctionalized Janus particles at the microscale has seen considerable research interest in the last years,<sup>[6d,7b,8a,9]</sup> fewer reports exist on nanoscale Janus particles.<sup>[10]</sup> Like the particles themselves, this challenge presents two separate faces: first, the initial realization of the Janus aspect by generating two

separate sides; second, the utilization of orthogonal methods that allow highly selective functionalizations of the respective hemispheres. The process of introducing two separate faces on particles has been realized by methods such as spray coating, metal vapor deposition, polymer-based phase separation, and/or microfluidic systems based on biphasic polymer chemistry, all summarized in recent reviews.<sup>[10,11]</sup> Many of these strategies rely on the deposition of particles on planar substrates, which inherently allow production of only very limited quantities of particles.<sup>[3a]</sup> While some polymer-based methods are able to produce Janus particles in large quantities, very specific polymers like block-copolymers are utilized, and the resulting soft nanoparticles often lack the flexible surface chemistry of inorganic nanoparticles.<sup>[6a,12]</sup> For hard particles, the Pickering wax emulsion technique introduced by Granick and co-workers is a particularly promising method in terms of scalability and yield.<sup>[6d,13]</sup>

Face-selective functionalization usually starts with equipping the surface with specific functional groups via sol-gel chemistry and related methods,<sup>[14]</sup> or by creating a single patch of a different material on the nanoparticle surface.<sup>[5d,8a,15]</sup> The functional groups then serve as moieties for (bio)molecules that are to be grafted onto the respective sides. Here, click chemistry of either the azide-alkyne copper or the thiol-maleimide varieties are the most widely used techniques for protein functionalization<sup>[7a]</sup> on Janus particles and are superior in specificity to the otherwise regularly used carbodiimide-based

---

R. Kadam, M. Zilli, Dr. M. Maas, Prof. K. Rezwan  
Advanced Ceramics  
University of Bremen  
Am Biologischen Garten 2, 28359 Bremen, Germany  
E-mail: michael.maas@uni-bremen.de  
Dr. M. Maas, Prof. K. Rezwan  
MAPEX Centre of Materials and Processes  
University of Bremen  
28359 Bremen, Germany

coupling methods. High specificity is especially critical for protein-functionalization at the nanoscale due to the general stickiness of particles and proteins at this size range.<sup>[16]</sup> Moreover, care needs to be taken to avoid or to mitigate the formation of a noncovalently bound protein corona, which can rapidly form at nanoparticle interfaces in the presence of biological media.<sup>[17]</sup>

As of yet, only few reports exist on dual biofunctionalization of Janus particles, most of them utilizing particles at the micrometer to sub-micrometer scale. At the lower end of the size spectrum, Lee and Yu prepared 500 nm silica Janus particles using a microcontact printing procedure with azide functionalized SiNPs followed by side-specific antibody attachment via amine-carboxylate carbodiimide chemistry. The covalently attached antibodies were thereafter shown to selectively target CD3 and CD25 receptors on T-cells.<sup>[4]</sup> Tang et al. prepared bifunctional 2.0–4.5  $\mu\text{m}$  silica and polystyrene Janus particles using a metal deposition technique followed by the orthogonal approaches of carbodiimide chemistry and biotin–streptavidin binding for protein functionalization at the respective faces.<sup>[7b]</sup> Similarly, Bradley et al. presented 850 nm Janus particles with multiple clickable polystyrene and poly(propargyl acrylate) sides using thiol-yne click chemistry for conjugation. Here, the initial face separation was realized via the seed emulsion technique.<sup>[18]</sup> Honneger and co-workers prepared 1  $\mu\text{m}$  polystyrene and silica particles which were partially coated with gold using a metal evaporation technique to introduce the Janus character.<sup>[19]</sup> An even smaller number of reports exist that describe the preparation of inorganic Janus particles with dual biofunctionalization at the nanoscale.<sup>[13f,14,20]</sup> Sánchez et al. used the wax Pickering emulsion technique to prepare 100 nm silica particles with single gold patches and then attached horseradish peroxidase on the silica face and biotin on the gold face.<sup>[13f]</sup> Villalonga et al. presented a similar preparation technique using mesoporous silica particles with a gold face for the controlled release of the dye tris(2,2-bipyridyl) ruthenium(II) chloride.<sup>[20]</sup> Zhang et al. described a preparation technique using polystyrene instead of wax, and prepared 150 nm silica Janus particles with conjugated proteins using click chemistry.<sup>[14]</sup> López et al. again used the wax-emulsion technique to prepare mesoporous silica Janus nanoparticles ( $d = 160$  nm) with folic acid and triphenylphosphate using carbodiimide chemistry for dual targeting of tumor cells and mitochondria.<sup>[8b]</sup> Since detection of proteins with transmission electron microscopy (TEM) can be difficult, in the paper by López et al., the Janus aspect was verified by adsorbing ultrasmall gold nanoparticles to the aminated hemisphere before biofunctionalization. Similarly, the other mentioned papers mostly describe successful preparation of nanoscale Janus particles as proof-of-principle for specific applications.<sup>[4,8b,13a,b,d,e,21]</sup>

In our study, we designed a general approach for the preparation of nanoscale (below 100 nm) Janus particles with dual protein functionalization to establish a platform for the synthesis of such particles with a wide variety of proteins. Specifically, we chose proteins that could be easily visualized in TEM in order to straightforwardly elucidate success and limitations of our approach. To this end, we synthesized biofunctionalized Janus particles by combining and extending several well-known techniques. We used 80 nm silica nanoparticles modified with an azidosilane surface to prepare Pickering emulsions using molten wax as the droplet phase.<sup>[13a]</sup>

The presence of the azide groups on the SiNPs enables the subsequent use of click chemistry. The azide functionalized SiNPs on the Pickering emulsion droplets were further subjected to face-selective silanization with biotin-polyethylene glycol (PEG) ethoxy silane. Afterward, we grafted ferritin on the azide-functionalized side via a click reaction and the biotin groups were conjugated with streptavidin, which was labeled with ultrasmall gold nanoparticles (Figure 1). Ferritin, which contains an iron oxide core, and gold-labeled streptavidin were primarily selected for their visibility in transmission electron microscopy and can in principle be substituted by many other proteins via click chemistry on one side and by using biotin-conjugated proteins to bind to streptavidin on the other side. To prove the existence of Janus particles in a quantifiable way, we performed a full colloidal characterization of the particles including quantification of the surface groups, dynamic light scattering (DLS) and TEM. Since DLS does not provide information on the distribution of proteins on the particle surface and the statistics of TEM analysis are generally poor, we also characterized the collective behavior of the Janus nanoparticles in dispersion by investigating the viscoelastic properties of thin films of particles adsorbed at the air/water interface. All measurements were repeated for 150 nm silica particles to confirm the general applicability of the method.

## 2. Results and Discussion

### 2.1. Preparation of Azidosilane-Functionalized Particles

The first step of our preparation strategy is the functionalization of SiNPs with an azidosilane using an established sol-gel coating method.<sup>[7a]</sup> The particle size before functionalization is  $80 \pm 20$  nm with fairly low polydispersity (PDI = 0.15). After functionalization, the size of the particles is  $90 \pm 10$  nm and some agglomerates can be observed (PDI = 0.26). The success of surface functionalization can be mainly assessed via a change in zeta potential (ZP) of the NP surface; here, the presence of azide groups on the surface of SiNPs ( $\text{R-N} = \text{N}^+ = \text{N}^-$ ) should neutralize the surface potential. Immobilization of azide groups on 80 nm SiNPs yielded a net negative charge of  $-25 \pm 2$  mV, which is moderately less negative compared to the nonfunctionalized particles ( $-37 \pm 3$  mV). The moderate change in ZP indicates that most of the SiNP surface is still covered by  $\text{OH}^-$  groups, which is also indicated by our quantitative analysis of surface groups (see the discussion below). Figure 2A,B shows representative TEM micrographs of the azide-SiNPs. See Table 1 for an overview of the prepared particles and their sizes, polydispersity, and ZPs.

### 2.2. Preparation of Wax-Water Pickering Emulsions

In the next step, the azide-functionalized particles were adsorbed at the surfaces of emulsion droplets of molten wax at 80 °C using the method first described by Granick and co-workers.<sup>[13a]</sup> Adsorption proceeds via the well-known Ramsden–Pickering effect<sup>[22]</sup> that leads to a decrease in surface free energy upon adsorption of particles at the liquid–liquid droplet

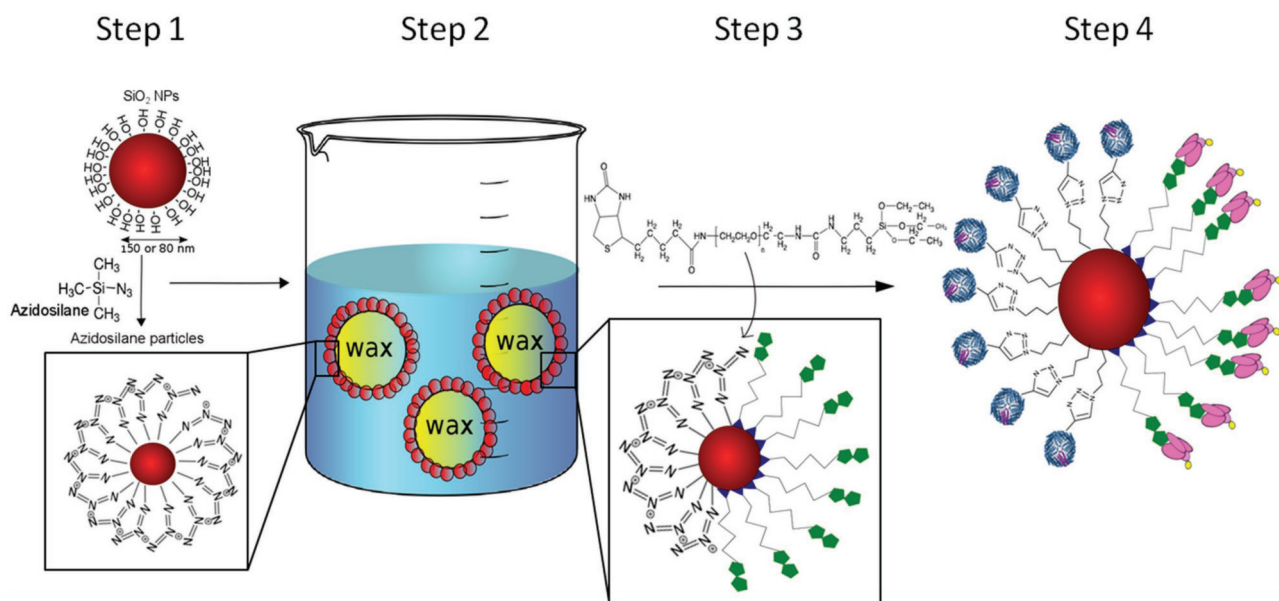
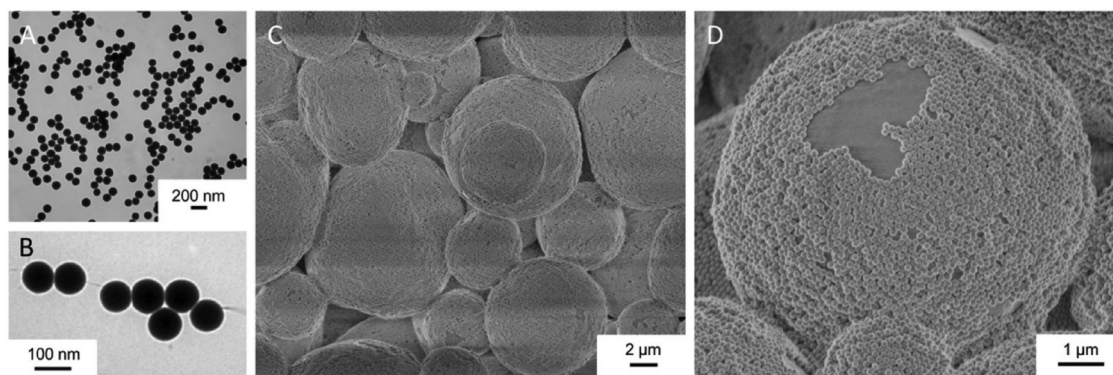


**Figure 1.** Schematic representation of the synthesis route of Nanoscale Janus particles with dual protein functionalization. Step 1: Unfunctionalized SiNPs were coated with azidosilane. Step 2: Formation of a wax-in-water Pickering emulsion stabilized by the azidosilane-functionalized particles and the surfactant CTAB. Step 3: The emulsion droplets are functionalized with biotin-PEG silane (green) and the wax was further dissolved to yield a Janus nanoparticle dispersion in MES buffer. Step 4: Janus particles with azide and biotin groups are functionalized with the proteins ferritin (blue) and gold-conjugated streptavidin (pink), respectively.

interface, but only if the particles are able to be wetted by both liquid phases. In order to realize adsorption of the highly hydrophilic silica particles, they were coated with the positively charged surfactant cetyltrimethylammonium bromide (CTAB) to increase their hydrophobicity.<sup>[13a]</sup> Due to the high surface area of the nanoscale particles, the surfactant concentration in the silica/wax/water dispersion had to be significantly increased compared to the original protocol, directly proportional to the actual surface area of the particles. After cooling of the emulsion to room temperature (RT), and with that solidifying of the Pickering emulsion droplets, the nanoparticle-covered wax microparticles have been analyzed via scanning electron microscopy (SEM) (Figure 2C,D). The wax microspheres showed sizes between 10 to 60  $\mu\text{m}$  with an irregular monolayer of azide-SiNPs on the surface that was able to withstand the filtration and

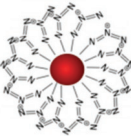
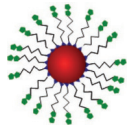
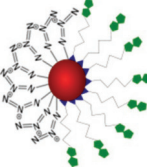
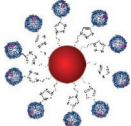
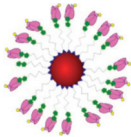
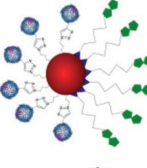
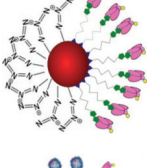
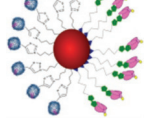
washing steps that were necessary to remove excess surfactant. Note that the nanoparticles were only lightly embedded in the wax, despite the strongly hydrophobic CTAB coating (Figure 2D). Since this method easily allows the production of these microparticles in gram quantities, it is a scalable approach for the production of Janus particles.

By firmly adsorbing at the wax droplet surfaces, the nanoparticles are partially masked against functionalization from the wax phase which allowed the modification of the water-facing surface using biotin-PEG silane, again via a simple sol-gel coating procedure in ethanol at ambient temperature. Here, an excess of the biotin-PEG silane ensured that an adequate amount of biotin groups covered the exposed azide functionalized particle surface. Since this ethanol-based method might cause harm to the wax microparticles, we again investigated



**Figure 2.** A,B) TEM micrographs of the prepared azidosilane-functionalized nanoparticles. C) SEM micrograph of wax-water Pickering emulsion stabilized by azide particles and the surfactant CTAB. D) Close-up view of a wax core stabilized with monolayer of azidosilane-functionalized particles.

**Table 1.** Size and ZP analysis of the 80 nm SiNPs after the applied functionalization steps. Functionalization of the respective hemispheres is marked by a dash.

Nanoparticle surface functionalization	Nanoparticle type	Zeta potential [mV]	Size average $d$ [nm]	PDI
Unfunctionalized		$-37.3 \pm 3$	$80 \pm 20$	0.15
Azidosilane (control)		$-25.2 \pm 2$	$90 \pm 10$	0.26
Biotin-PEG silane (control)		$-4.4 \pm 0.5$	$160 \pm 6$	0.14
Janus azidosilane/biotin-PEG silane		$-11.3 \pm 2$	$92 \pm 15$	0.22
Azidosilane-ferritin (control)		$-27.3 \pm 5$	$165 \pm 25$	0.33
Biotin-PEG silane-streptavidin (control)		$+18.1 \pm 6$	$80 \pm 25$	0.25
Janus azidosilane-ferritin/biotin-PEG silane		$-17.1 \pm 5.5$	$145 \pm 68$	0.15
Janus azidosilane/biotin-PEG silane-streptavidin		$+7.6 \pm 2.3$	$96 \pm 50$	0.18
Janus azidosilane-ferritin/biotin-PEG silane-streptavidin		$+18.3 \pm 6$	$156 \pm 20$	0.21

the morphology of the wax spheres using SEM after the modification of the spheres with biotin-PEG silane (Figure S1, Supporting Information). After sol-gel coating, the wax spheres tend to shed some SiNPs from their surface. However, a majority of the particles remained, ensuring the success of the functionalization of the water-exposed SiNP face with biotin

groups. The partial dissolving of wax in some areas during the reaction and, subsequently, several washing steps to wash off any residual silane molecules, might be the reason for the loss of the SiNPs from the wax droplet surfaces. We already optimized this coating method for maintaining the integrity of the nanoparticle-covered wax microspheres. Experiments with methanol, toluene, longer reaction times, and slightly elevated reaction temperatures proved unsuccessful (data not shown).

After side-selective functionalization of the SiNPs with biotin-PEG silane, cyclohexane was used to dissolve the wax cores and hence to release the SiNPs with azide and biotin groups on their respective sides. After wax removal, these Janus SiNPs were observed to be less negatively charged ( $-11.3 \pm 2$  mV) compared to the homogeneously azidosilane-functionalized SiNPs. This trend was also confirmed with fully (nonJanus) biotin-functionalized 80 nm particles ( $-4.4 \pm 0.5$  mV). Due to their low zeta-potential, the Janus particles were only slightly agglomerated ( $92 \pm 15$  nm, PDI 0.22) which was also observed in case of the 150 nm Janus NPs (Table S2, Supporting Information).

The number of biotin and azide surface groups was quantified using the Fluoreporter biotin quantification kit and the fluorescence of DBCO-Cy3, respectively. We attained a much higher number of biotin groups on the SiNPs compared to the number of azide groups (Figure 3; Figure S3, Supporting Information). An analysis of the azide groups using the DBCO-Cy3 fluorometric analysis yielded only  $8.03 \pm 2.3$  groups per fully azide-coated 80 nm SiNP (Figure 3). An average of  $63.6 \pm 7.3$  azide groups was found on each fully azide-coated 150 nm SiNP (Figure S3, Supporting Information). Comparatively, 80 and 150 nm Janus particles with an azide-coated hemisphere presented only  $6.02 \pm 4.5$  and  $21.2 \pm 0.3$  azide groups per SiNP, respectively. This difference between the 80 and 150 nm particles correlates directly to the surface area ratio based on the two particle diameters of 3.5. The surprisingly low number of azide groups still provides sufficient moieties for the subsequent click reaction as described below and are also reflected in the minor change in ZP as discussed above, as well as in the patchy binding with ferritin as shown below. Using the Fluoreporter Biotin quantification kit, an average of  $6430 \pm 44$  biotin groups on fully biotin-functionalized 80 nm SiNPs and of  $2009 \pm 12$  groups per 80 nm Janus SiNP were found (Figure 3). A similar evaluation of the 150 nm fully and half biotin-functionalized Janus particles yielded  $28260 \pm 25$  and  $8478 \pm 53$  groups, respectively (Figure S3, Supporting Information) which again closely represents the surface area ratio between these two particles. The high numbers of biotin moieties on the silica surface represent roughly 0.3 functional groups per  $\text{nm}^2$  of surface area, which shows that the surface is densely covered with biotin groups.

### 2.3. Preparation of Dual Biofunctional Janus NPs

The functionalization strategy with azide and biotin groups on the respective sides of the SiNPs enables orthogonal binding of proteins in further reaction steps. This we demonstrate with the model proteins ferritin and streptavidin. The azide groups can be utilized for the azide-acetylene cycloaddition click

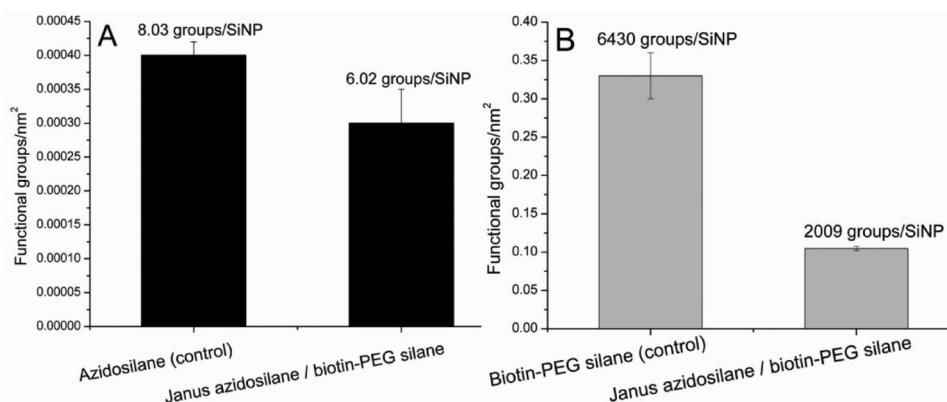


**Figure 3.** Number of biotin and azide functional groups per square nanometer on the surface of 80 nm nanoparticles. The number of available azide and biotin groups on the SiNPs was determined using the fluorescence of DBCO-Cy3 and of the Fluoreporter Biotin quantification kit, respectively. The numbers on the dark black and shaded bars represent the number of A) biotin and B) azide groups per SiNP. The fully coated SiNPs (first bar), were compared to the half functionalized Janus azidosilane-biotin PEG silane NPs (second bar).

reaction,<sup>[23]</sup> which is able to link proteins that are modified with an acetylene group. Here, we used acetylene-modified ferritin, which, owing to its iron-containing core, can be efficiently visualized using TEM. The protein immobilization strategy, which is compatible with proteins and avoids the use of harsh chemicals, is performed in  $10 \times 10^{-3}$  M 2-(*N*-morpholino)ethanesulfonic acid (MES) buffer (pH 6.1) at room temperature. The isoelectric point of ferritin of 5.5 imparts a slight negative charge to the nonJanus SiNPs after functionalization at the buffer pH of 6.1, which was confirmed by ZP measurements ( $-27.3 \pm 5$  mV) (see Table 1). Similarly, ferritin functionalization on the azidosilane/biotin-PEG Janus particles restores the negative charge of the nonprotein functionalized SiNPs from  $-11.3 \pm 2$  to  $-17 \pm 5$  mV. TEM analysis shows the presence of agglomerated ferritin patches on the 80 nm control particles (full azide functionalization, Figure S2A,B, Supporting Information) as well as on the Janus particles (Figure 4A–C). The origin of the patches is most likely the low surface density of azide groups as discussed above. Noncovalent adsorption of ferritin was ruled out by control experiments in the absence of the copper catalyst for the click reaction (data not shown). Uncontrolled protein adsorption onto nanoparticles, the well-known protein corona effect, can be attributed to the clustered iron cores that can be observed on all ferritin-conjugated particles (Figure 4A–C,G–I; Figure S4A–C,G–I, Supporting Information). In solution, ferritin is only slightly negatively charged ( $-1.62 \pm 0.2$  mV), which might further contribute to agglomeration between the protein molecules.

The other hemisphere of the Janus particle was biofunctionalized with biotin-PEG silane which was chosen to avoid unspecific interaction with proteins due to the PEG backbone and to ensure face-selective protein attachment via the highly specific biotin–streptavidin moiety. We used as-purchased streptavidin molecules that were conjugated to 10 nm gold particles to again ensure visibility in TEM and a good contrast to the iron oxide cores of ferritin. Functionalization with streptavidin was performed in  $10 \times 10^{-3}$  M MES buffer and was first tested for the nonJanus particles with full biotin-PEG coating (Figure S2, Supporting Information). These fully biotin-PEG coated 80 nm particles had a positive net charge

after streptavidin functionalization ( $+18.6 \pm 6$  mV,  $-4.4 \pm 0.5$  mV before coating). On the Janus particles, side-specific functionalization with streptavidin could be observed, as well (Figure 4D–F). Note, however, that some gold particles (for example seen on Figure 4F) could be observed on the azide-functionalized side of the Janus particles, as well, most likely caused by unspecific physisorption of streptavidin. As expected for only half a coating, the ZP is lower ( $+7.6 \pm 2.3$ ), while size and PDI remain stable, which indicates a stable dispersion. The 150 nm particles which were biofunctionalized in the same way as described here closely follow the same trends (see Table S1, Figures S2 and S4 in the Supporting Information).

Finally, Janus particles with dual protein faces were successfully prepared and the clear segregation of the ferritin and streptavidin sides is evident from the differences in iron and gold contrasts in the TEM micrographs (Figure 4G–I). Note, however, that the functionalization is not completely homogeneous, which is most likely a result of a varying immersion of the particles in the wax surface as well as multilayer formation on some parts of the wax surface. The dual biofunctionalized particles maintain their colloidal stability with only minor changes in PDI and some dimerization. The success rate of this face-wise two-step protein functionalization was determined by counting the number of Janus particles in the TEM micrographs of the samples with dual biofunctionalization. We observed that 24% of the 80 nm SiNPs were successfully coated with bifacially separated proteins, while 60% were Janus particles with only one protein and only 16% did not show any Janus aspect. The remaining particles were Janus particles with either ferritin or streptavidin coatings on one side (Table 2). In case of the 150 nm biofunctionalized Janus particles, the success rate for dual biofunctionalization was 28%, as summarized in Table S2 in the Supporting Information.

Along with the mentioned irregularities of the wax spheres, moderate agglomeration of the particles prior to protein immobilization may influence functionalization and hence may cause the decrease of the reported success rates. However, the observed dimerization (DLS sizes around 160 nm for 80 nm particles) is not necessarily connected to the Janus properties of the particles, as it was also observed in some of the

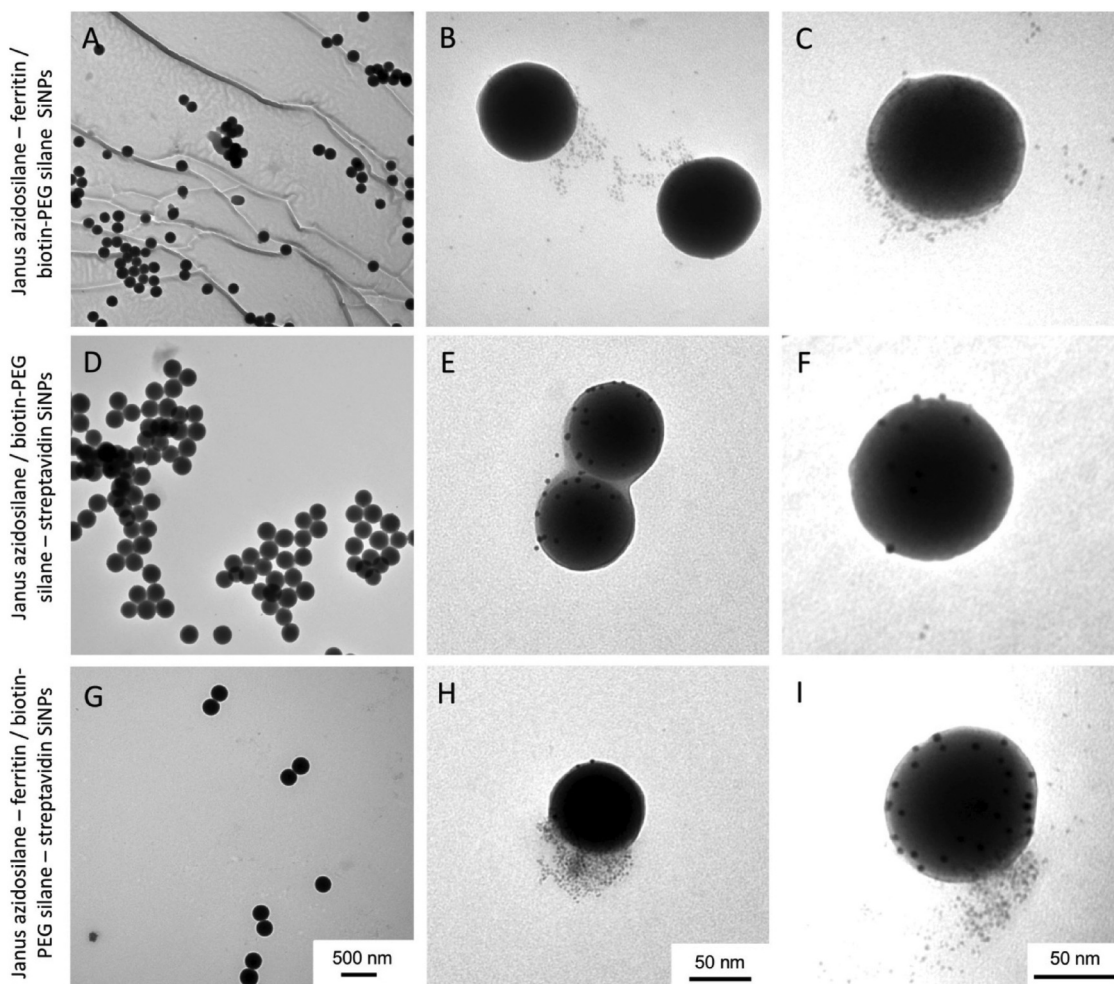


**Figure 4.** TEM images of the prepared 80 nm Janus particles functionalized with azidosilane on one side and biotin-PEG silane on the other side. The rows show A–C) the different combinations of protein conjugation, D–F) conjugated only with ferritin, G–I) only streptavidin and both proteins. Column (A, D, G) shows overview images, while the remaining images show close-ups of individual, representative particles. The scale bars in (G–I) apply to each image in the respective columns.

homogeneously functionalized controls (see Table 1). Additionally, some complications might arise as a result of incomplete dissolution of the wax causing particles to be trapped in residual wax, which might also prevent proper redispersion of the nanoparticles. This aspect might necessitate further process optimization in regard to the envisioned biological applications of these Janus particles.<sup>[7a]</sup>

**Table 2.** Success rate of protein functionalization of the 80 nm Janus particles. 50 random particles in each sample from three separate samples were examined and counted manually using TEM to assess the success of the preparation technique.

Name	Number	[%]
Janus azidosilane ferritin/biotin-PEG silane–Streptavidin	12 ± 6	24 ± 12
Janus azidosilane/biotin-PEG silane–streptavidin	10 ± 3	20 ± 6
Janus azidosilane–ferritin/biotin-PEG silane	20 ± 4	40 ± 8
Not biofunctionalized	8 ± 1	16 ± 2

#### 2.4. Pendant Drop Tensiometry

In order to characterize the collective behavior of the Janus particle dispersions, pendant drop tensiometry was used to measure the interfacial tension of the various Janus nanoparticles over periods of several hours at the air/MES–buffer interface (Figure 5A). Additionally, the interfacial dilatational rheology of the droplet interface was characterized by oscillating the droplet volume and recording the complex 2D elasticity of the surface (Figure 5B). The number of particles chosen for the analysis was maintained at 10 mg mL<sup>-1</sup>, which is more than sufficient for populating the full droplet surface. The aqueous MES buffer showed a surface tension of 69 mN m<sup>-1</sup> which was not significantly changed by the presence of unfunctionalized (black) and nonbiofunctionalized Janus SiNPs (green), indicating that the highly hydrophilic SiNPs themselves are not surface active.<sup>[24]</sup> The freely dissolved proteins ferritin and gold-conjugated streptavidin were highly surface active (Figure S5A, Supporting Information), as is well documented for various other proteins.<sup>[25]</sup> Here, ferritin seems to have a slightly stronger

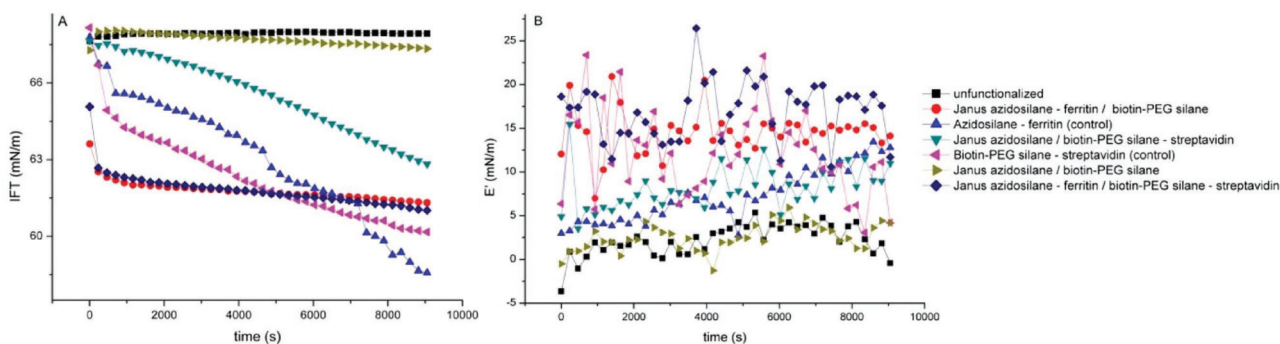


**Figure 5.** Interfacial tension and elastic storage modulus versus time using a pendant drop tensiometer for the 80 nm SiNPs. 0.1 M MES buffer was used as the drop phase. A) Average interfacial tensions recorded at the air–water interface. B) The 2D storage module  $E'$  of the droplet interface at a constant frequency of  $1\text{ s}^{-1}$  and an amplitude ( $dA/A$ ) of 1%. See Figures S5–S7 in the Supporting Information or the complete data of all investigated particles and proteins.

effect when compared to streptavidin-gold. They both form highly elastic interfacial films (Figure S5B, Supporting Information) as is evidenced by the high 2D storage modulus  $E'$ , which again has a typical value for proteins.<sup>[25]</sup> Based on the surface activity of the conjugated proteins, the protein-coated particles are all observed to decrease interfacial tension. Accordingly, the fully protein-coated SiNPs (pink and bright blue) are more surface active compared to their half protein counterparts (green and red). Following the trend for the free proteins, half and fully ferritin-functionalized SiNPs show a stronger effect compared to the streptavidin functionalized controls (Figure 5A). This is also reflected in the 2D elastic module (Figure 5B) and viscous module (Figure S6, Supporting Information) of the dilatational rheological measurements. The dual biofunctionalized Janus particles (dark blue) are highly surface active compared to nonfunctionalized SiNPs (black). While the interfacial tension of dual biofunctionalized Janus particles is comparable to that of the half ferritin coated SiNPs (red) (Figure 5A), the surface elasticity of the dual biofunctionalized particles is the highest of all analyzed particles (Figure 5B), showing that the Janus aspect influences the collective behavior of the particles at the air/water interface. All measurements were repeated for 150 nm Janus SiNPs with comparable results besides an even more strongly pronounced surface activity of the dual biofunctionalized particles (Figure S7, Supporting Information).

### 3. Conclusion

In summary, our results suggest that the chosen approach is a versatile platform for the face-selective immobilization of two different biomolecules on a single nanoparticle surface. This scalable method yields Janus nanoparticles in gram quantities and is compatible for functionalization of biomolecules such as proteins with well-established protein functionalization strategies at mild conditions. However, due to the iterative process with some losses in specificity at every step, only adequate success rates for functionalization with two proteins could be achieved. Still, the Janus particle dispersion shows collective properties that clearly surpass those of Janus particle dispersions with only one protein. These features will enable further studies on interactions between Janus nanoparticles and cells

or other biological systems and could also be utilized in biomedical applications that benefit from dual functionalities on separate sides of a nanoparticle.<sup>[13]</sup>

### 4. Experimental Section

**Materials—General Chemicals and Devices:** Silica nanoparticles (product number SIOP010-01-100G) from FiberOptic Center (New Bedford, USA), paraffin wax (product number 8002-74-2) with a melting point between 75 and 90 °C from Merck Millipore (Darmstadt, Germany), 3-azidopropyltriethoxysilane (azidosilane, product number AB268770) from ABCR GmbH (Karlsruhe, Germany), dibenzylcyclooctyne-Cy3 (DBCO-Cy3 product number 920) from Biomol GmbH (Hamburg, Germany), Fluoreporter Biotin Quantification Assay Kit (product number. F30751) from Invitrogen (Karlsruhe, Germany) and ethoxy-PEG- Biotin silane 3400 (product no. 145-40) from Laysan Bio Inc (Alabama, USA) were purchased. MES (product no. 011M8418), copper (II) sulfate pentahydrate ( $\text{CuSO}_4$ , product no. 7758-99-8), L-ascorbic acid (product no. A92902), and hexadecyltrimethylammonium bromide (CTAB, product no. 855820) were all purchased from Sigma Aldrich (Munich, Germany). Double deionized water ( $\text{ddH}_2\text{O}$ , conductivity less than  $<0.4\ \mu\text{S cm}^{-1}$ ) was used for all investigations (SynergyUltra Water System Millipore Corp., Massachusetts, USA).

**Materials—Proteins:** Ferritin from equine spleen (product number. F4503) from Sigma Aldrich (Munich, Germany), and Streptavidin gold conjugate (1 mL, OD10) (product no. AC-10-04-15) was purchased from CytoDiagnostics (Ontario, Canada).

**Methods—Surface Functionalization of Silica NPs:** SiNPs (both 80 and 150 nm) were functionalized with azide groups using the protocol described in<sup>[7a]</sup>. 0.5 mL of ethanol containing 21  $\mu\text{L}$  azidosilane was mixed with 9 mL of SiNP suspension in water (8.7 mg/mL). This mixture was subjected to continuous stirring at RT for 60 min and then heated to 90 °C for another 60 min at 700 rpm. The particles were washed three times using centrifugation and resuspension steps to remove excess of unreacted silanes. The particles were dried at 70 °C overnight and used for experiments as required.

**Methods—Preparation of Janus Particles:** A paraffin wax-in-water emulsion was prepared in batches of 50 mL adapting the protocol described by the Granick group who first introduced it.<sup>[13a]</sup> 140 mg of 80 nm azide SiNPs were homogeneously dispersed in water. 2 mg CTAB was added to this mixture to partially hydrophobize the NPs by physisorption. 1 g of wax is then added to this dispersion. This entire setup was heated to a temperature of 80 °C to melt the wax, and an emulsion was prepared using an Ultra Turrax homogenizer at 9500 rpm for 90 s. This setup was allowed to cool down for the solidification of the wax. The solidified wax droplets were then washed three times with water using vacuum filtration to remove excess of CTAB and unbound NPs.

10 mg of the Pickering emulsion droplets were further dispersed in 9 mL absolute ethanol. 1 mL of 8 mg mL<sup>-1</sup> biotin-PEG ethoxy silane solution in ethanol was slowly added to this mixture under N<sub>2</sub> bubbling conditions at room temperature for 2 h. This amount corresponds to approximately nine times a monolayer of silane molecules related to the total SiNP surface area. The functionalized Pickering emulsion droplets were then washed thrice with ethanol to remove any silane residues. The morphology of these Pickering emulsion droplets was confirmed by SEM (Figure S1, Supporting Information). Cyclohexane was added to these wax droplets overnight at ambient temperature to dissolve the wax. The particles were extracted using 10 × 10<sup>-3</sup> M MES buffer. The prepared NPs were immediately used for protein conjugation purposes.

**SiNP Protein Conjugation:** The formed particles were centrifuged at 3000 rpm for 3 min to remove excess of agglomerated SiNP. Three centrifugation and redispersion cycles were used to wash the particles. The final supernatant was used as the final particle suspension for the protein conjugation purposes. The particle concentration used in every protein conjugation step was 10 mg mL<sup>-1</sup>. The protein conjugation steps were performed in a two-step method. Ferritin, which is attached via copper mediated click chemistry to the azide side, was functionalized with an acetylene group using the protocol described in ref. [26]. The particles were dispersed in 2 mL of 10 × 10<sup>-3</sup> M MES buffer, and then incubated with 10 μL of streptavidin-gold for 2 h at 4 °C to enable protein bioconjugation with biotin. As stated by the manufacturer, each 10 nm gold NP is decorated with 20 streptavidin molecules. SiNP conjugated with ferritin and streptavidin-gold were further washed with 10 × 10<sup>-3</sup> M MES buffer thrice using centrifugation and redispersion steps as done previously. Finally, the particles were dispersed in 2 mL of fresh 10 × 10<sup>-3</sup> M MES buffer.

**Janus NP Characterization—Stability and Particle Morphology:** Size and ZP measurements were performed using 10 mg mL<sup>-1</sup> SiNP dispersions in 10 × 10<sup>-3</sup> M (pH 6.1) using a DLS device (ZetaSizer NanoSP, Malvern, United Kingdom). Wax Pickering emulsion droplets were visualized before and after functionalization using SEM (Supra 40-Carl Zeiss, Germany). Morphologies of the NPs before and after each protein functionalization step were visualized using transmission electron microscopy (TEM-EM 900, Carl Zeiss, Germany). For SEM and TEM analysis, a droplet of the dispersion was placed on a silicon wafer or a copper grid (Plano GmbH, Wetzlar, Germany), respectively, and allowed to dry in air. The samples did not require sputter coating.

**Janus NP Characterization—Quantification of Functional Surface Groups:** The SiNP functionalized with azide and biotin groups were used for quantification of the specific groups using DBCO-Cy3 and Fluoreporter Biotin quantification kits, respectively. The azide group quantification was performed using the protocol described in ref. [7a]. The particles were washed three times using MilliQ water to remove unspecifically bound dye by repeated centrifugation at 12 000 rpm for 20 min and redispersion using ultrasonic bath. The fluorescence of the bound Cy3 was determined by excitation at 553 nm and emission at 563 nm using the spectrometer plate reader (CHAMELEON V, Hidex, Finland). Biotin groups were determined on the Janus SiNP according to the product specification sheet. All samples were analyzed in triplicates and the values are plotted in terms of average ± standard deviation.

**Janus NP Characterization—Manual Counting of Bifunctional Protein-Janus NPs:** Four microliters of an aqueous dispersion (1 mg mL<sup>-1</sup>) of the prepared protein functionalized Janus NPs from three separate batches were deposited on different copper grids and visualized using TEM. Fifty randomly selected particles from each batch were analyzed for the presence of non-, mono- and bifunctional protein conjugated SiNPs, both for the 80 and 150 nm particles. The results have been summarized in Table 2; Table S2 in the Supporting Information.

**Janus NP Characterization—Pendant Drop Tensiometry:** The changes in the interfacial tension ( $\gamma$ ) of the dispersion of Janus particles at a buffer-air interface was measured using pendant drop tensiometry (OCA25, DataPhysics, Filderstadt, Germany) over a specific period of 2.5 h. In order to study the viscoelastic properties of the biofunctionalized Janus NPs, movies of the oscillating drop formed at the tip of a small steel capillary were recorded and the changes in the interfacial tension over time were used to calculate values of storage modulus (or elastic

modulus)  $E'$ , which is the real part of the complex surface elasticity  $E^*$  and loss modulus (or viscous modulus)  $E''$ , which is the imaginary part of  $E^*$ . An 8 μL drop of 10 mg mL<sup>-1</sup> NP dispersions in 10 × 10<sup>-3</sup> M MES buffer was created at the tip of the capillary (size  $\varnothing$  of 0.5 mm) and oscillated at an amplitude  $dA/A$  of 1% and a frequency of 1 Hz over a period of 2.5 h.

Controls experiments included pure 10 × 10<sup>-3</sup> M MES buffer, nonfunctionalized SiNPs, half and fully coated ferritin functionalized SiNPs in combination with and without gold-conjugated streptavidin and were analyzed in triplicates. As positive controls, similar concentrations of both pure proteins in the absence of SiNPs were also analyzed in triplicates. Representative graphs are shown in favor over a statistic evaluation of the results since the systematic error is generally higher than the statistical error in such measurements. Measurements with the same particles were almost congruent.

## Supporting Information

Supporting Information is available from the Wiley Online Library or from the author.

## Conflict of Interest

The authors declare no conflict of interest.

## Keywords

click chemistry, janus nanoparticles, protein functionalization, silane, silica, sol gel

- [1] P. G. de Gennes, *Science* **1992**, *256*, 495.
- [2] a) L. Y. Wu, B. M. Ross, S. Hong, L. P. Lee, *Small* **2010**, *6*, 503; b) H.-Y. Hsieh, T.-W. Huang, J.-L. Xiao, C.-S. Yang, C.-C. Chang, C.-C. Chu, L.-W. Lo, S.-H. Wang, P.-C. Wang, C.-C. Chieng, C.-H. Lee, F.-G. Tseng, *J. Mater. Chem.* **2012**, *22*, 20918.
- [3] a) J. Suh, D. Wirtz, J. Hanes, *Proc. Natl. Acad. Sci. USA* **2003**, *100*, 3878; b) B. Brandenburg, L. Y. Lee, M. Lakadamyali, M. J. Rust, X. Zhuang, J. M. Hogle, *PLOS Biol.* **2007**, *5*, e183.
- [4] K. Lee, Y. Yu, *J. Mater. Chem. B* **2017**, *5*, 4410.
- [5] a) M. A. Fernandez-Rodriguez, Y. Song, M. A. Rodriguez-Valverde, S. Chen, M. A. Cabrerizo-Vilchez, R. Hidalgo-Alvarez, *Langmuir* **2014**, *30*, 1799; b) M. A. Fernandez-Rodriguez, L. Chen, C. P. Deming, M. A. Rodriguez-Valverde, S. Chen, M. A. Cabrerizo-Vilchez, R. Hidalgo-Alvarez, *Soft Matter* **2016**, *12*, 31; c) N. Glaser, D. J. Adams, A. Boker, G. Krausch, *Langmuir* **2006**, *22*, 5227; d) I. Schick, S. Lorenz, D. Gehrig, A. M. Schilman, H. Bauer, M. Panthofer, K. Fischer, D. Strand, F. Laquai, W. Tremel, *J. Am. Chem. Soc.* **2014**, *136*, 2473.
- [6] a) L. Treccani, T. Yvonne Klein, F. Meder, K. Pardun, K. Rezwan, *Acta Biomater* **2013**, *9*, 7115; b) H. M. Ding, Y. Q. Ma, *Nanoscale* **2012**, *4*, 1116; c) S. M. Janib, A. S. Moses, J. A. MacKay, *Adv. Drug Delivery Rev.* **2010**, *62*, 1052; d) J. Zhang, B. A. Grzybowski, S. Granick, *Langmuir* **2017**, *33*, 6964.
- [7] a) M. C. Lo Giudice, F. Meder, E. Polo, S. S. Thomas, K. Alnahdi, S. Lara, K. A. Dawson, *Nanoscale* **2016**, *8*, 16969; b) J. L. Tang, K. Schoenwald, D. Potter, D. White, T. Sulchek, *Langmuir* **2012**, *28*,

- 10033; c) C. M. Niemeyer, *Angew. Chem., Int. Ed.* **2001**, *40*, 4128; d) Z. Nie, W. Li, M. Seo, S. Xu, E. Kumacheva, *J. Am. Chem. Soc.* **2006**, *128*, 9408.
- [8] a) B. Chen, Y. Jia, Y. Gao, L. Sanchez, S. M. Anthony, Y. Yu, *ACS Appl. Mater. Interfaces* **2014**, *6*, 18435; b) V. Lopez, M. R. Villegas, V. Rodriguez, G. Villaverde, D. Lozano, A. Baeza, M. Vallet-Regi, *ACS Appl. Mater. Interfaces* **2017**, *9*, 26697; c) Y. Yi, L. Sanchez, Y. Gao, K. Lee, Y. Yu, *Chem. Mater.* **2017**, *29*, 1448; d) K. Lee, Y. Yu, *J. Mater. Chem. B* **2017**, *5*, 4410.
- [9] B. Li, M. Wang, K. Chen, Z. Cheng, G. Chen, Z. Zhang, *Macromol. Rapid Commun.* **2015**, *36*, 1200.
- [10] Y. Yi, L. Sanchez, Y. Gao, Y. Yu, *Analyst* **2016**, *141*, 3526.
- [11] a) M. Lattuada, T. A. Hatton, *Nano Today* **2011**, *6*, 286; b) A. Walther, A. H. Muller, *Chem. Rev.* **2013**, *113*, 5194.
- [12] X. C. Pang, C. S. Wan, M. Y. Wang, Z. Q. Lin, *Angew. Chem., Int. Ed.* **2014**, *53*, 5524.
- [13] a) L. Hong, S. Jiang, S. Granick, *Langmuir* **2006**, *22*, 9495; b) A. Perro, F. Meunier, V. Schmitt, S. Ravaine, *Colloids Surf., A* **2009**, *332*, 57; c) R. Villalonga, P. Diez, A. Sanchez, E. Aznar, R. Martinez-Manez, J. M. Pingarron, *Chemistry* **2013**, *19*, 7889; d) A. Zenerino, C. Peyratout, A. Aimable, *J. Colloid Interface Sci.* **2015**, *450*, 174; e) C. Kaewsaneha, P. Tangboriboonrat, D. Polpanich, M. Eissa, A. Elaissari, *ACS Appl. Mater. Interfaces* **2013**, *5*, 1857; f) A. Sánchez, P. Díez, P. Martínez-Ruíz, R. Villalonga, J. M. Pingarrón, *Electrochem. Commun.* **2013**, *30*, 51.
- [14] J. Zhang, X. Wang, D. Wu, L. Liu, H. Zhao, *Chem. Mater.* **2009**, *21*, 4012.
- [15] M. Guix, A. K. Meyer, B. Koch, O. G. Schmidt, *Sci. Rep.* **2016**, *6*, 21701.
- [16] C. A. Batista, R. G. Larson, N. A. Kotov, *Science* **2015**, *350*, 1242477.
- [17] M. P. Monopoli, C. Aberg, A. Salvati, K. A. Dawson, *Nat. Nanotechnol.* **2012**, *7*, 779.
- [18] L. C. Bradley, K. J. Stebe, D. Lee, *J. Am. Chem. Soc.* **2016**, *138*, 11437.
- [19] T. Honegger, S. Sarla, O. Lecarme, K. Berton, A. Nicolas, D. Peyrade, *Microelectron. Eng.* **2011**, *88*, 1852.
- [20] R. Villalonga, P. Díez, A. Sánchez, E. Aznar, R. Martínez-Máñez, J. M. Pingarrón, *Chem. - Eur. J.* **2013**, *19*, 7889.
- [21] a) A. Kirillova, L. Ionov, I. V. Roisman, A. Synytska, *Chem. Mater.* **2016**, *28*, 6995; b) G. Rucinskaite, S. A. Thompson, S. Paterson, R. de la Rica, *Nanoscale* **2017**, *9*, 5404.
- [22] S. U. Pickering, *J. Chem. Soc., Trans.* **1907**, *91*, 2001.
- [23] J. L. Brennan, N. S. Hatzakis, T. R. Tshikhudo, N. Dirvianskyte, V. Razumas, S. Patkar, J. Vind, A. Svendsen, R. J. Nolte, A. E. Rowan, M. Brust, *Bioconjug. Chem.* **2006**, *17*, 1373.
- [24] a) K. Hanni-Ciunel, N. Schelero, R. von Klitzing, *Faraday Discuss.* **2009**, *141*, 41; b) R. McGorty, J. Fung, D. Kaz, V. N. Manoharan, *Mater. Today* **2010**, *13*, 34.
- [25] A. V. Makievski, V. B. Fainerman, M. Bree, R. Wüstneck, J. Krägel, R. Miller, *J. Phys. Chem. B* **1998**, *102*, 417.
- [26] A. Gole, C. J. Murphy, *Langmuir* **2008**, *24*, 266.